Photochemical Reactions of Photosystem II in Ethylene Glycol[†]

Warwick Hillier,*[,‡] Philip Lukins,[§] Michael Seibert,[||] and Tom Wydrzynski[‡]

Research School of Biological Sciences, The Australian National University, Canberra, ACT 0200, Australia, School of Physics, University of Sydney, NSW 2006, Australia, and Basic Sciences Center, National Renewable Energy Laboratory, Golden, Colorado 80401

Received July 15, 1996; Revised Manuscript Received September 18, 1996[⊗]

ABSTRACT: The behavior of photosystem II (PSII) reactions was investigated under conditions of decreasing water content by the addition of increasing concentrations of ethylene glycol (EG). The photosynthetic activities were measured for PSII samples either directly in aqueous solutions of EG or in the standard buffer medium following EG treatment. Several effects on PSII arise upon exposure to EG. Below 50% EG there are no significant irreversible changes, although there is a slowing of the Q_A^- reoxidation kinetics in the presence of EG. At concentrations of 50−70% EG, protein structural changes occur that include the release of the 16, 23, and 33 kDa extrinsic proteins and two of the catalytic Mn ions. For these samples, the capacity for O_2 evolution is considerably reduced and the formation of donor side H_2O_2 is enhanced. In 60% EG, the nanosecond components in the rate of $P680^+$ reduction are converted entirely to microsecond kinetics which upon return of the sample to the standard buffer medium are partially restored, indicating that EG has a reversible, solvent effect on the PSII donor side. At concentrations of EG >70% chlorophyll fluorescence measurements reveal reversible increases in the F_O level concomitant with the generation and disappearance of a 5 μs decay component in the $P680^+$ reduction kinetics. This result may indicate a solvent-induced uncoupling of the light harvesting pigment bed from the reaction center complex. As the EG concentration is increased to 80−100%, there is an irreversible loss of the primary charge separation. The use of EG as a cryoprotectant and as a water-miscible organic solvent for PSII is discussed.

Photosystem II (PSII)[1] is the membrane-bound protein complex that performs the unique water oxidation chemistry which generates molecular oxygen for the biosphere. The water oxidation reaction is driven by the capture of light energy at a special photoactive chlorophyll molecule, P680, and is catalyzed by a cluster of four manganese ions. The arrangement of the four Mn ions in the oxygen evolving complex (OEC) is unknown but is suggested to be a pair of electronically coupled Mn dimers (Yachandra et al., 1993), although it is still unclear whether or not they are magnetically coupled (Smith & Pace, 1996). The Mn cluster is situated towards the lumenal side of the PSII complex (Hansson & Wydrzynski, 1990; Pokorny et al., 1994) and is probably ligated to several amino acids of the reaction center protein D1 (Preston & Seibert, 1991a,b; Nixon & Diner, 1992; Boerner et al., 1992; Chu et al., 1994a,b, 1995a,b).

Several proteins appear to be essential for the complete oxidation of water to molecular oxygen and include the reaction center proteins D1, D2, and cytochrome b_{559}, the chlorophyll-*a* binding proteins CP43 and CP47, a 33 kDa extrinsic protein, and several other low-molecular-weight polypeptides (Debus, 1992). The targeted deletion of any one of these proteins either eliminates or greatly reduces the O_2 evolution activity, indicating that they have an important role in the mechanism of water oxidation. The D1 protein is clearly involved in the ligation of the Mn ions, but the function of the other proteins is less certain. One possible role for these proteins may be to create a structurally-intact hydrophobic domain around the Mn cluster that is needed to optimize O_2 formation (Thompson et al., 1989; Wydrzynski et al., 1996).

The release of O_2 follows a four-step reaction pattern (Joliot et al., 1968) that is described by the well-known S_n-state cycle (where $n = 0, 1, 2, 3, 4$) (Kok et al., 1970). In this model, the OEC advances one oxidation step following each photo-excitation, beginning in the S_1 state after dark adaptation. Upon reaching the S_4 state, O_2 is released and the OEC resets to the S_0 state to begin the cycle again.

The nature of the water oxidation mechanism has been addressed by many groups, yet the binding of the substrate water during the S_n-state cycle and the reaction sequence by which the O−O bond is formed remain unknown. Recent rapid isotope exchange measurements using ^{18}O-labeled water have identified very different binding properties for

[†] This work was supported in part by a grant from the Australian Research Council (P.L.) and by the Energy Biosciences Division, Office of Basic Energy Sciences, U.S. Department of Energy (M.S.). The National Renewable Energy Laboratory is operated by the Midwest Research Institute for the U.S. Department of Energy under Contract DE-AC36-83CH10093. W.H. and T.W. appreciate travel support from NREL.

* Author to whom correspondence should be addressed. E-Mail: Hillier@RSBS-Central.anu.edu.au.

[‡] The Australian National University.

[§] University of Sydney.

[||] National Renewable Energy Laboratory.

[⊗] Abstract published in *Advance ACS Abstracts*, November 15, 1996.

[1] Abbreviations: DCMU, 3-(3,4-dichloro)-1,1-dimethyleurea; DMAB, 3-(dimethylamino)benzoic acid; EG, ethylene glycol (treated); EGW, ethylene glycol treated and returned to aqueous medium; HEPES, 4-(2-hydroxyethyl)-1-piperazineethanesulfonic acid; HMD, H_2O_2 assay based on the reagents **H**RP−**M**BTH−**D**MAB; HRP, horseradish peroxidase; MBTH, 3-methyl-2-benzothiazolinone hydrazone; MES, 2-(*N*-morpholino)ethanesulfonic acid; P680, the chlorophyll primary electron donor molecule; Pheo, the pheophytin primary electron acceptor molecule; PSII, photosystem II; Q_A and Q_B, first and second plastoquinone electron acceptors, respectively; Y_Z and Y_D, tyrosine electron donor molecules.

S0006-2960(96)01724-2 CCC: $14.00

the two substrate H_2O molecules in the S_3 state (Messinger et al., 1995). These findings suggest that the chemical environment of the two substrate water molecules in the OEC is different and may imply that the entry of water into the catalytic reaction sequence is regulated by the surrounding protein matrix (Wydrzynski et al., 1996). In terms of classical chemical kinetics, however, little is known about the true K_M for water oxidation because the substrate is also the solvent and remains at exceptionally high concentrations, approaching 55 M.

A novel way to investigate the enzymatic properties of the water oxidation reaction would be to develop a nonaqueous solvent system for PSII. Substrate control could then be achieved through the addition of limited amounts of water. Previous work has shown that nonaqueous solvent systems can be developed for other enzyme systems, resulting in novel changes in the substrate specificity, reaction products, and reaction rates (Zacs & Kilbanov, 1985; Dordick, 1989). To date, the use of nonaqueous solvents has usually been applied to small hydrophilic enzymes. The organic solvents used in these studies are mostly unsuitable for PSII as they solubilize the bound chlorophyll pigments and inactivate PSII function. However, there is one group of solvents, the polyols (e.g., glycerol, ethylene glycol), that do not significantly extract the chlorophyll pigments and are commonly used with PSII preparations as stabilizing agents (Steward & Bendall, 1981) or as cryoprotectants (Farkas & Malkin, 1979; Apostolova et al., 1994). The suitability of polyols for PSII studies is enhanced further since they are completely miscible with water. Thus, the polyols can potentially be used for the study of the water oxidation reactions.

In the present work we have used ethylene glycol (EG) as a water-miscible organic solvent for PSII and have investigated its effects as a function of increasing concentration. In an earlier investigation, the effect of EG was determined only on the total activity of PSII (Inoue & Nishimura, 1971). Here we report the effects of EG on various PSII partial reactions as well as on the protein and Mn content. Chlorophyll fluorescence and 830 nm absorption transient measurements were used to determine the rates of Q_A^- reoxidation and $P680^+$ reduction, respectively, both in the presence of EG and when the sample had been returned to the standard buffer medium after EG treatment. Our findings indicate that EG has an array of effects on PSII function that are due to both electronic and structurally-induced interactions.

MATERIALS AND METHODS

Sample Preparation. Photosystem II membrane fragments were prepared from hydroponically-grown spinach according to Berthold et al. (1981). Thylakoid membranes were treated for 10 min with 5% (v/v) Triton X-100. The solubilized PSII membrane fragments were then collected by centrifugation and washed twice (300 mL total volume) with a standard buffer medium consisting of 20 mM MES (pH 6.0), 400 mM sucrose, 15 mM NaCl, and 5 mM $MgCl_2$ and stored at −80 °C.

Ethylene Glycol Treatment. Treatment of thawed PSII samples was performed by adding the sample directly to the EG solution and incubating at a Chl concentration of 250 μg mL^{-1} for 20 min in the dark immediately prior to measurement. At low EG concentrations there was no problem to add PSII samples directly into the EG solution, but at high EG concentrations (above 90%) the samples had to be first pelleted by centrifugation and then resuspended in a solution at the appropriate EG concentration. Samples that required return to the standard buffer medium were centrifuged and then resuspended. These samples are denoted as EGW-treated samples. All EG treatments were performed at room temperature.

Steady-State PSII Activity Assays. Steady-state PSII activity assays were performed using EGW-treated samples. Oxygen evolution was measured with a Hansatech O_2 electrode at 25 °C using saturating red light (>2000 μmol m^{-2} s^{-1}), with 10−20 μg of Chl in 1 mL of standard buffer medium (pH 6.0) containing 0.4 mM *p*-phenylbenzoquinone (PPBQ) and 0.5 mM $K_3Fe(CN)_6$ as electron acceptors.

The photoreduction of 2,6-dichlorophenolindophenol (DCPIP) using diphenylcarbazide (DPC) as the electron donor was determined from the light-induced absorption change at 600 nm (Seibert et al., 1989) measured on a Shimadzu UV-3000 difference absorption spectrophotometer. Saturating red actinic light (>1200 μmol m^{-2} s^{-1} in the sample cuvette) was provided by a 100 W xenon lamp equipped with a Corion LG-650 long wave filter. The detector was shielded with a Corion 600 nm interference filter. The reaction mixture contained 50 μM DCPIP, 200 μM DPC in the standard buffer medium plus 10 μg of Chl (mL of sample)$^{-1}$. The molar extinction coefficient for oxidized DCPIP at pH 6.0 was derived from Armstrong (1964).

The light-induced generation of H_2O_2 by PSII was detected spectrophotometrically using a horseradish peroxidase (HRP) coupled reaction between 3-methyl-2-benzothiazolinone hydrazone (MBTH) and 3-(dimethylamino)benzoic acid (DMAB) (Hillier & Wydrzynski, 1992). Light-induced absorption changes at 600 nm were measured under the same experimental conditions as for the DPC-DCPIP assay. The reaction mixture contained the standard buffer medium at pH 7.0 (20 mM HEPES was used instead of MES), 0.1 mM MBTH, 5 mM DMAB, 0.25 mM 2,6-dimethyl-*p*-benzoquinone (DMBQ-6), 3 units of HRP, and a sample concentration of 10 μg of Chl mL^{-1}.

Mn Quantification. Bound Mn was solubilized from PSII by acidification of the sample in 300 mM HCl. The Mn content was then determined from the relative amplitude of the room temperature, six-line Mn EPR signal in comparison with a standard curve. Measurements were performed with a Bruker ESP 300E spectrometer (X-band, 9.5 GHz). The operating conditions were: 20 mW microwave power; 100 kHz modulation frequency; 16 G modulation amplitude; 655 ms time constant; 1×10^5 gain.

Protein Gel Electrophoresis. Protein composition was determined by denaturing SDS−PAGE using a modified discontinuous gel system (Ikeuchi & Inoue, 1988) containing 600 mM Tris-HCl (pH 6.8) and 7.5 M urea. The sample material was solubilized for at least 1 h in the solubilizing buffer (5% LiDS, 7.5 M urea, 60 mM Tris-HCl, pH 6.8, and 10% glycerol) prior to loading. The gels were run overnight at 20 mA, stained with Coomassie brilliant blue R-250, dried, and scanned with a densitometer.

Chlorophyll Fluorescence Measurements. The chlorophyll fluorescence levels for open (F_O) and closed (F_M) reaction centers were measured with a PAM101 modulated fluoro-

meter. The F_O level was determined using low intensity, 1.6 kHz LED pulses (1 μs duration, $\lambda = 650$ nm), and F_M was attained following a 2 s saturating actinic light pulse.

The fluorescence decay transients were measured after a single saturating flash with a home-built (flash probe) modulated LED fluorometer (Ghirardi et al., 1996). Weak probing pulses (10 kHz) were provided by a 625 nm LED array filtered with a LS-650 filter. Fluorescence was detected by a photodiode/RG-715 filter combination. The actinic flash was supplied by a xenon flash lamp (3 μs half-width) filtered through a Schott BG-18 filter. Variable probe modulation was controlled by the data acquisition software. All measurements were made at a sample concentration of 13 μg of Chl mL^{-1} in the presence of 12 μM 3-(3,4-dichloro)-1,1-dimethyleurea (DCMU). The samples were incubated for 20 min in the dark at room temperature. Upon switching on the modulation beam, the fluorescence increased to a level, F_{eq}, which was slightly greater than the F_O level. The data are thus presented as $(F - F_{eq})/(F_{eq})$. The fluorescence decay kinetics were analyzed using a nonlinear least-squares curve-fitting algorithm contained in the application Sigma Plot (Jandel Scientific).

830 nm Absorption Transient Measurements. The kinetics of $P680^+$ reduction were measured at 830 nm using a single-beam transient absorption instrument (Lukins et al., 1996). Samples were excited by <4 ns FWHM Gaussian pulses at 532 nm from a frequency-doubled Q-switched Nd:YAG laser (Continuum Surelite-20), and the induced absorption change at 830 nm was probed using a temperature-tuned CW single-mode GaAlAs diode laser (SDL-5412). The transmitted infrared was detected by an avalanche photodiode (Hamamatsu S2383-01). The resulting signal was amplified by a 500 MHz preamplifier and the transient recorded on a LeCroy 9361 digital oscilloscope. Sample fluorescence and other unwanted contributions to the signal were reduced to undetectable levels using glass, interference, and spatial filters. Sampling rates of 2.5 and 1 GS/s were used for nanosecond measurements while 100 and 5 MS/s were used for microsecond measurements. A sample chlorophyll concentration of 40 μg mL^{-1} was used in a medium consisting of 50 mM HEPES (pH 7.2), 300 mM mannitol, 10 mM $MgCl_2$, and 10 mM $CaCl_2$ together with 2 mM $K_3Fe(CN)_6$ as an electron acceptor. This medium was found to optimize the absorption signal and to stabilize the sample (Völker et al., 1989; Lukins, unpublished). The double-washed PSII samples contained lower detergent levels than usual and consequentially had higher scattering. Although the S/N was reduced under these conditions, the effects of EG were not complicated by the presence of detergent.

The amplitude of the initial absorption change saturated at an excitation pulse energy of ~1.2 mJ. We used a slightly greater energy (1.5 mJ) to ensure saturation. Measurements were performed after a 5 min dark equilibration period in the cuvette. Signals were averaged over 50 laser pulses given at a repetition rate of 2 Hz. Addition of 5 mM NH_2OH led to the commonly observed conversion from nanosecond to microsecond kinetics. The transients were analyzed using a nonlinear least-squares curve-fitting routine in the application Sigma Plot.

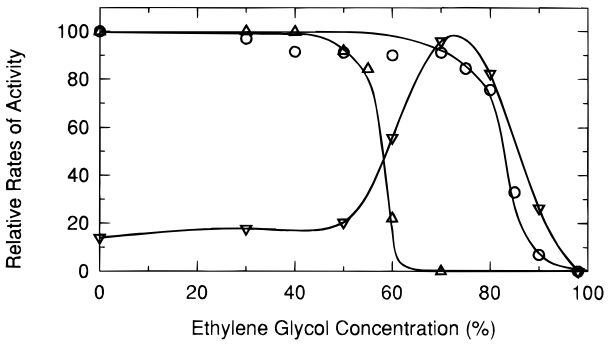

FIGURE 1: The relative rates of O_2 evolution (△), DPC-DCPIP photoreduction (○), and H_2O_2 formation (▽) of photosystem II samples as a function of ethylene glycol exposure. Samples were treated in solutions of ethylene glycol/standard buffer medium for 20 min at ambient room temperature and then returned to the standard buffer medium for assay. Maximum rates: O_2 evolution, 400 μmol (mg of Chl)$^{-1}$ h^{-1}; DPC-DCPIP photoreduction, 130 μmol (mg of Chl)$^{-1}$ h^{-1}; H_2O_2 formation, 46 μmol (mg of Chl^{-1}) h^{-1}.

RESULTS

O_2 Evolution and DCPIP Photoreduction. The rates of O_2 evolution after a 20 min exposure to increasing concentrations of EG and return of the sample to the standard buffer medium (i.e., EGW-treated samples) are shown in Figure 1. The activity remains essentially unaffected up to 50% EG. Above 50% EG, O_2 evolution rapidly drops and after exposure to 65% EG it is a totally inactivated. These results are similar to those reported earlier (Inoue & Nishimura, 1971).

The narrow concentration range (55−65% in EGW-treated samples) where O_2 evolution declines is strongly influenced by the duration of EG exposure. Although no time dependence was found at EG concentrations below 55%, at 60% EG the treated sample had rates that were initially high but declined to a stable level (~20% of the control) after a 20 min incubation. Longer incubation times yielded only negligible differences in the remaining activity. At 4 °C, the inactivation by EG was slowed down and relatively high rates of O_2 evolution could be measured even at 75% EG (data not shown).

To obtain information on the intrinsic capacity for primary photochemistry in PSII, the rates of 2,6-dichlorophenolindophenol (DCPIP) photoreduction in the presence of the electron donor diphenylcarbazide (DPC) were determined. These results are also shown in Figure 1 for EGW-treated samples and indicate that the loss in O_2 evolution occurs at significantly lower EG concentrations than the loss in photochemistry. The rate of the DPC-DCPIP reaction exhibits no decline until a concentration of 70% EG is attained, while at this concentration O_2 evolution is completely inactivated. In the range 75−90% EG, DPC-DCPIP photoreduction declines and there is no observable activity upon exposure to 100% EG.

Protein and Mn Loss. To examine why PSII samples exhibit such a rapid decline in O_2 evolution upon exposure to intermediate concentrations of EG, protein analysis by SDS−PAGE was undertaken. As shown in Figure 2A, exposure to EG at concentrations below 50% has no effect on the extrinsic proteins; however, at higher concentrations the extrinsic proteins are released with a clear correlation to the loss in O_2 evolution activity over the 55−65% range. A

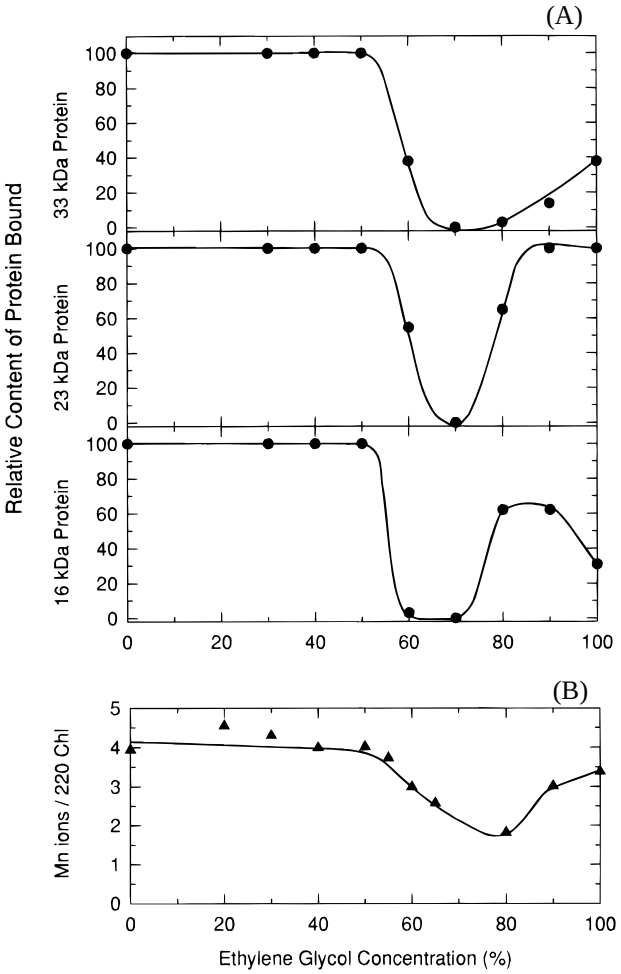

FIGURE 2: Protein and Mn loss from photosystem II samples following exposure to increasing concentrations of ethylene glycol. Protein dissociation (A) was quantified by densitometry of the SDS−PAGE gel patterns. Release of Mn (B) was determined by EPR and quantified by comparison to a standard curve. Values are based upon a photosynthetic unit size of 220 Chl per reaction center.

surprising finding is that at EG concentrations greater than 70% there is only a partial release of the extrinsic proteins. In particular, at 100% EG, only ~60% of the 16 and 33 kDa proteins and none of the 23 kDa protein is released. The dissociation behavior of the extrinsic proteins was independent of the sample chlorophyll concentration, indicating that the retention of the proteins under these conditions was unlikely to be due to protein rebinding.

Loss of the extrinsic proteins, particularly of the 33 kDa protein, is known to destabilize the Mn complex (Yamamoto et al., 1981; Kuwabara & Murata, 1982). In order to determine how the Mn cluster is affected by EG, we determined the Mn content after EG treatment. As shown in Figure 2B, the progressive loss of two of the catalytic Mn ions over the 55−65% EG concentration range correlates with the loss of the 33 kDa protein (Figure 2A) and inactivation of O_2 evolution (Figure 1). This result is in agreement with the general concept that the 33 kDa protein provides a stabilizing action on the Mn cluster and that the loss of only two Mn ions is sufficient to inactivate O_2 evolution (Ono & Inoue, 1984; Miyao & Murata, 1984; Seibert et al., 1988). It is known that addition of high concentrations of Ca^{2+} and Cl^- ions can retard the release of the two Mn ions in 33 kDa protein depleted samples (Ono & Inoue, 1984; Bricker, 1992); however, the presence of 10 mM $CaCl_2$ had no effect on O_2 evolution activity in our measurements (data not shown). It is interesting to point out that at 100% EG most of the Mn remains bound to PSII.

HMD Detected H_2O_2 Generation. Release of the extrinsic proteins from PSII has been correlated with increases in the formation of H_2O_2 (Schröder & Åkerlund, 1986; Berg & Seibert, 1987; Hillier & Wydrzynski, 1993). Steady-state rates of H_2O_2 generation were thus measured in EGW-treated samples using a spectrophotometric assay developed earlier (Hillier & Wydrzynski, 1993), and the results are shown in Figure 1. In general, the rates of H_2O_2 formation increase as the O_2 evolution decreases. At 75% EG, the rate reaches a maximum which is ~6-fold greater than the control, i.e., 46 μmol of H_2O_2 (mg of Chl)$^{-1}$ h^{-1} vs 8 μmol of H_2O_2 (mg of Chl)$^{-1}$ h^{-1} and then declines at higher EG concentrations, parallelling the loss in the DPC-DCPIP reaction. There is no H_2O_2 generation in 100% EGW-treated samples.

Chlorophyll Fluorescence Measurements. Changes in the chlorophyll fluorescence yield from PSII provide a noninvasive probe for the intrinsic capacity for charge separation. The fluorescence level is determined by the redox states of Q_A and P680 [reviewed by Dau (1994)]. In dark-adapted samples, reaction centers are open and the fluorescence level (F_O) is low due to the presence of the fluorescence quencher Q_A. Upon formation of the charge-separated state, $P680^+$ Q_A^-, the reaction center closes to further excitation. The fluorescence level arising from a closed reaction center initially remains low due to the quenching properties of $P680^+$, but as $P680^+$ is reduced by the electron donor Y_Z ($t_{1/2}$ = 30 ns: Mauzerall, 1972; Brettel et al., 1984) a high fluorescence state (F_M) is achieved, i.e., Y_Z^+ P680 Q_A^-. The fluorescence level F_M is 2−5-fold greater than the F_O level. The increase in fluorescence level from F_O to F_M is due to a decrease in the rate constant for charge separation that occurs as the pool of Q_A becomes reduced under continuous illumination (Schatz et al., 1988; Roelofs et al., 1992). This is interpreted to arise from the electrostatic field of Q_A^- which interacts with the electron accepting properties of the pheophytin molecule (Schatz et al., 1988).

The ratio F_V/F_M is indicative of the photochemical efficiency for an open PSII reaction center. In an intact system, F_V/F_M approaches a maximum value of 0.83. The F_V/F_M values for PSII in the presence of EG and for EGW-treated samples are shown in Figure 3A. As with the measurements of O_2 evolution, protein release, and Mn content, there is no effect of EG on F_V/F_M at concentrations below 50%. Interestingly, in the 50−60% range there is still no effect. The F_V/F_M only declines in the 60−90% range, where the decline is not as rapid as the loss in O_2 evolution (Figure 1). At 90% EG, all variable fluorescence is eliminated. For EGW-treated samples, the behavior is not much different than for samples in the presence of EG.

The F_O fluorescence levels for samples in EG and EGW-treated samples are shown in Figure 3B. Changes in the F_O level reflect a malfunction of the PSII reaction center possibly due to a loss in the energy transfer efficiency from the light harvesting pigment bed (Osmond, 1994). The results in Figure 3B show virtually no change in the F_O level for EGW-treated samples, but in the presence of EG there is a significant rise over the 60−80% concentration range. In 100% EG the F_O level undergoes a dramatic increase, to a level 6-fold higher than in the control. The fact that the F_O

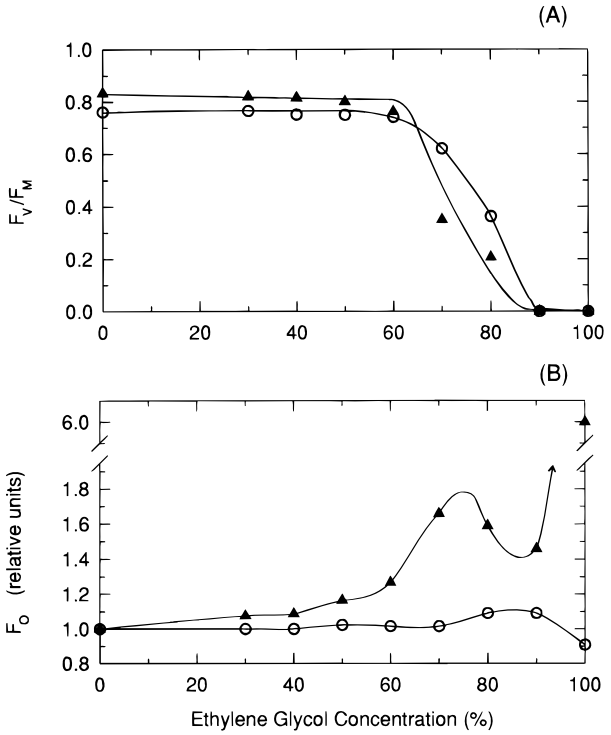

FIGURE 3: Chlorophyll fluorescence parameters for photosystem II samples as a function of ethylene glycol exposure. (A) F_V/F_M ratio for samples in ethylene glycol solutions (▲) and for samples returned to the standard buffer medium (○). (B) F_O level for samples in ethylene glycol solutions (▲) and for samples returned to the standard buffer medium (○). The F_O level was normalized to that of the control level.

remains constant for the EGW-treated samples over the entire concentration range indicates the EG effect on F_O is reversible.

Q_A^- Charge Recombination Reactions. Flash-probe measurements of the chlorophyll-*a* fluorescence decay kinetics are used to determine the rate of Q_A^- reoxidation and to provide information regarding the mechanisms of electron transfer in the PSII reaction center. Normally, Q_A^- oxidation is dominated by the forward electron transfer reaction to the secondary quinone acceptor Q_B ($t_{1/2} = 100-200$ μs: Robinson & Crofts, 1983), but for samples with DCMU present where the forward reaction to Q_B is blocked, the rate of Q_A^- oxidation becomes dependent upon recombination reactions. The main recombination reaction occurs between Q_A^- and $P680^+$, with the concentration of $P680^+$ being determined by the equilibrium between P680 and various PSII electron donors; i.e.

Scheme 1

$$S_nY_ZP680^+ \underset{k_{-1}}{\overset{k_1}{\rightleftharpoons}} S_nY_Z{}^+P680 \underset{k_{-2}}{\overset{k_2}{\rightleftharpoons}} S_{(n+1)}Y_ZP680$$

Thus, the rate of Q_A^- recombination will depend on the presence or absence of an oxidizable Mn cluster. For PSII samples without photooxidizable Mn, the rate is the fastest since the concentration of $P680^+$ is determined only by the ratio (k_{-1}/k_1), while in an intact system the rate is slower because the concentration of $P680^+$ becomes a function of both (k_{-1}/k_1) and (k_{-2}/k_2) (Buser et al., 1992; Nixon & Diner, 1992). In the situation when modulating pulses are used to measure fluorescence, the S_n states are scrambled so that k_{-2} is an average rate constant (mainly from S_2 and S_3).

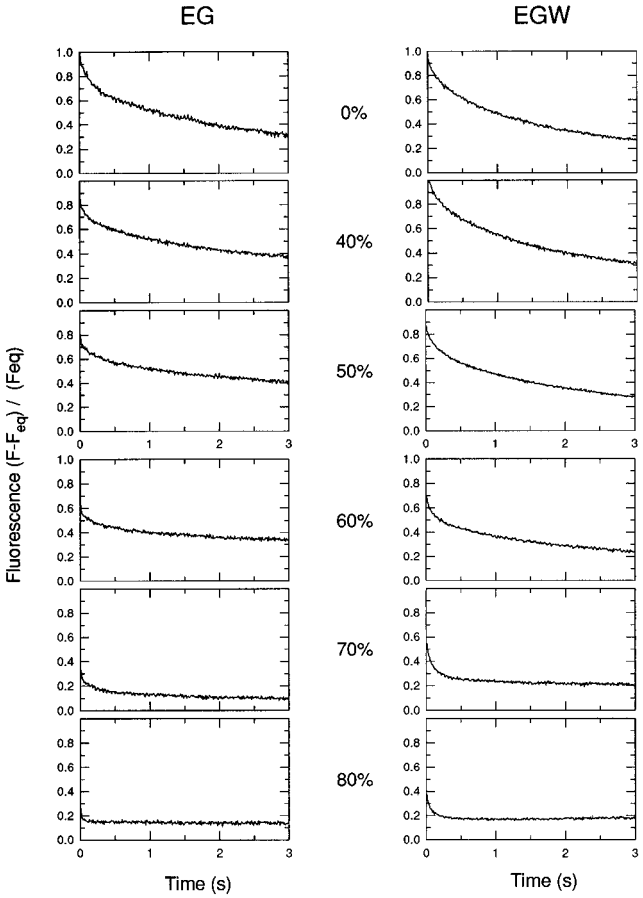

FIGURE 4: Chlorophyll fluorescence decay curves of photosystem II samples in response to a saturating flash as a function of increasing ethylene glycol exposure. Samples were treated in ethylene glycol solutions (EG: left column) and returned to the standard buffer medium (EGW: right column). 12 μM DCMU was included in the assay medium. The transients begin ~120 μs after the flash.

The fluorescence decay transients for PSII samples in the presence of increasing EG concentrations and for EGW-treated samples are presented in Figure 4, and the calculated lifetimes are given in Table 1. The decay transients for the control and for samples treated with EG below 60% were fitted with three exponential decay components. Transients for samples treated at 70% and 80% EG required the introduction of a long-lived decay component and had to be fitted using either two (at 70% EG) or one (at 80% EG) exponential decay component plus a constant. The three components of the control sample have lifetimes of 110 ms (19%), 1.04 s (33%), and 5.6 s (49%). For the samples in the presence of EG over the 30−50% range, there is an increase in the lifetime for the third component. The slowing in the fluorescence decay is not apparent when the samples are returned to the standard buffer medium (i.e., the EGW-treated samples), which suggests that this effect is a reversible, solvent-specific interaction. The formation of the long-lived component at 70−80% EG is unlikely to be due to the oxidation of Y_D or Cyt b_{559} as these components are oxidized with very low quantum yields (Buser et al., 1990, 1992).

830 nm Transient Absorption Measurements. Primary charge separation in the PSII reaction center occurs in ~3 ps (Wasielewski et al., 1989; Seibert, 1993) with the formation of the radical pair $P680^+Pheo^-$. This is immediately followed by a rapid charge-stabilization event with

Table 1: Kinetic Components of the Chlorophyll Fluorescence Decay for PSII Samples Exposed to Ethylene Glycol (EG) and for Samples Then Returned to Standard Buffer Medium (EGW)[a]

	EG exposure			EGW exposure		
solvent concn (%)	rel amplitude (%)	lifetime (s)	yield at 120 μs	rel amplitude (%)	lifetime (s)	yield at 120 μs
0	19	0.11	1.01	14	0.12	1.00
	33	1.04		37	0.83	
	49	5.6		49	5.0	
30	14	0.09	0.99	17	0.09	0.99
	38	1.07		38	0.95	
	48	6.2		45	6.4	
40	16	0.08	0.92	16	0.08	0.86
	25	0.73		21	0.58	
	59	6.7		64	4.38	
50	16	0.09	0.87	16	0.09	0.81
	20	0.68		23	0.70	
	64	8.1		55	5.0	
60	23	0.05	0.61	23	0.08	0.70
	26	0.45		21	0.68	
	51	9.8		57	5.91	
70	44	0.06	0.36	48	0.07	0.56
	22	0.81		14	0.86	
	33	>100		38	>100	
80	67	0.05	0.36	52	0.09	0.36
	33	>100		47	>100	

[a] The data represent an average of three measurements. Samples were measured at 13 μg of Chl mL^{-1} in the presence of 12 μM DCMU.

the reduction of the nearby quinone molecule Q_A ($t_{1/2} = 300-500$ ps: Nuijs et al., 1986; Schatz et al., 1987), thus forming the state $P680^+Q_A^-$. The formation of $P680^+$ results in the bleaching of the Chl absorption peak at 680 nm and a broad absorption increase in the near infrared centered at 830 nm (van Gorkom et al., 1975). By monitoring the 830 nm absorption decay, the kinetics of $P680^+$ reduction can be directly obtained (van Best & Mathis, 1978). The nanosecond components of this decay are dependent on the S_n states, exhibiting a progressive slowing with advancing S_n state (Brettel et al., 1984). Under multiple-flash conditions, where the S_n states are randomized, two principal nanosecond components exist, with pH-dependent lifetimes (Meyer et al., 1989). The remaining decay occurs with microsecond half-lives of 1, 5, 35, and 130 μs (Brettel & Witt, 1984). The slowest microsecond component is attributed to $P680^+Q_A^-$ charge recombination.

The inset in Figure 5 shows a typical nanosecond transient for the 830 nm absorption change of our control samples. The nanosecond decay comprises about 75% of the total signal and can be resolved into two exponential components with half-lives of 31 ± 3 and 100 ± 7 ns. As these values did not change significantly with increasing EG concentration, they were fixed to obtain the relative amplitude for each component which were then combined to provide the total nanosecond contribution. The kinetic analysis for EG- and EGW-treated samples is reported in Tables 2 and 3, respectively.

The extents of the nanosecond contribution to $P680^+$ reduction for EG- and EGW-treated samples are shown in Figure 6. Samples treated in EG undergo a total loss of nanosecond kinetics upon exposure to 60% and higher concentrations, with the onset of inhibition occurring at about 30% EG. The loss in the nanosecond contribution is compensated by a corresponding increase in the total microsecond contribution over this EG range. Conversion

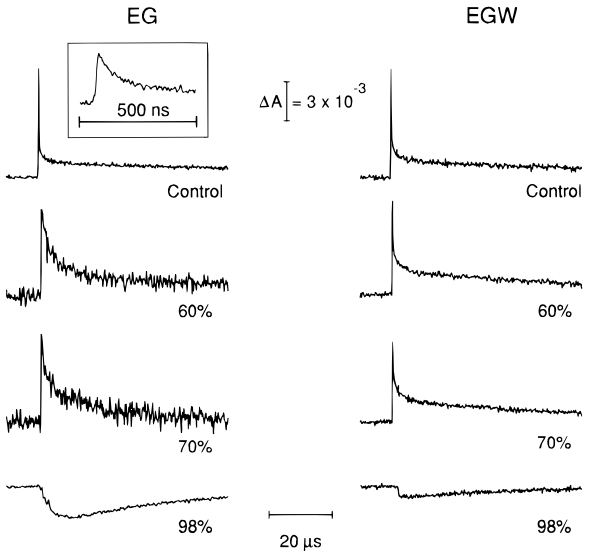

FIGURE 5: Transient absorbance changes at 830 nm over a 100 μs time frame for various EG- and EGW-treated photosystem II samples. Signals were averaged over 50 measurements. Inset shows the 830 nm absorbance change for a control sample over a 500 ns time frame. (A 7 point FFT smoothing was used on this transient.)

Table 2: Amplitudes of the Kinetic Components in the ΔA_{830nm} Change for PSII Samples Exposed to Various Concentrations of Ethylene Glycol (EG)[a]

EG concn (%)	A_1 (<1 μs)	A_2 (1 μs)	A_3 (5 μs)	A_4 (35 μs)	A_5 (130 μs)	ΣA (total)
0	76	10	0	10	4	100
20	66	11	0	7	3	87
30	62	10	1	6	6	85
35	47	14	1	20	3	85
40	37	23	4	29	3	96
45	33	21	9	32	2	97
50	18	22	36	18	6	100
60	0	50	24	10	9	93
65	0	43	19	21	5	88
70	0	31	27	17	0	75
80	0	5	40	32	5	82
90	0	12	9	25	14	60

[a] Half-lives are indicated in parentheses.

Table 3: Amplitudes of the Kinetic Components in the ΔA_{830nm} Change for PSII Samples Exposed to Ethylene Glycol and Returned to the Standard Buffer Medium (EGW)[a]

EGW concn (%)	A_1 (<1 μs)	A_2 (1 μs)	A_3 (5 μs)	A_4 (35 μs)	A_5 (130 μs)	ΣA (total)
0	75	13	0	7	5	100
20	77	12	0	6	5	100
30	67	9	1	6	5	88
40	66	11	0	1	4	82
50	56	10	2	15	4	85
55	52	15	0	12	1	80
60	40	22	2	17	5	86
70	0	48	0	26	6	80
80	0	34	0	21	7	62
90	0	23	0	0	4	27

[a] Half-lives are indicated in parentheses.

of nanosecond to microsecond kinetics is usually observed when O_2 evolution is inhibited (van Best & Mathis, 1978; Conjeaud & Mathis, 1980). An interesting comparison is made when the EG-treated samples are returned to the standard buffer medium. In this case, the nanosecond kinetics decline is shifted to a higher EG concentration range (40−70%). In particular, in 60% EG there is a complete

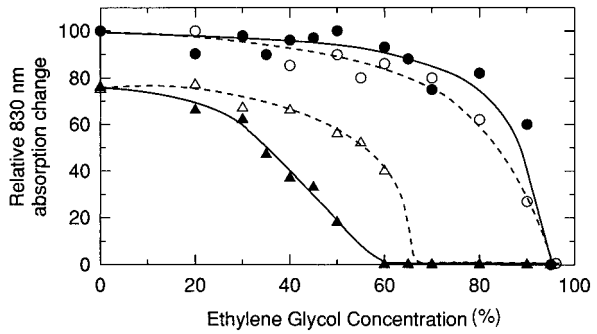

FIGURE 6: Relative nanosecond contribution (▲ △) and total amplitude (● ○) of the 830 nm absorbance signal for photosystem II samples in ethylene glycol solutions (solid lines and closed symbols) and then returned to the standard buffer medium (dotted lines and open symbols).

loss of the nanosecond kinetics; yet upon resuspension of the sample in the aqueous media, more than half of the nanosecond kinetics is restored, consistent with the combined O_2 evolution and H_2O_2 formation activities observed under this condition (Figure 1). The phenomenon indicates a reversible, solvent effect on the donor side components of PSII.

The total yields of $P680^+$ as determined from the initial signal amplitude of the 830 nm nanosecond transients are also plotted in Figure 6. From these results, it is clear that the primary charge separation remains largely unaffected by EG until concentrations above 70% are reached. The measurable activity then steadily declines to zero over the 70−95% range for both EG- and EGW-treated samples. The loss of $P680^+$ formation at high EG concentrations correlates with the loss of primary photochemistry as measured by DPC-DPCIP photoreduction (Figure 1) and F_V/F_M (Figure 3A).

The microsecond contribution to the $P680^+$ decay was determined from 830 nm transients measured out to 200 μs. In order to get more information on the conversion of the nanosecond kinetics to microsecond kinetics upon treatment with EG, the microsecond transients were analyzed for kinetic components. Four exponential decay components could be established from a free fit of the data for the control sample with half-lives of 1 μs (18%), 5 μs (<3%), 35 μs (10%), and 130 μs (7%).

The slowest component ($t_{1/2}$ =130 μs) generally comprises less than 10% of the total signal and is attributed to $P680^+Q_A^-$ recombination (Conjeaud & Mathis, 1986). This should not be confused with the slower phases of the fluorescence decay (also attributed to $P680^+Q_A^-$ recombination) as the quasi-steady-state equilibrium of $P680^+$ is determined by the PSII electron donors (Scheme 1). It was expected at first that the loss of the nanosecond contribution by EG treatment should result in an increase in the 130 μs component (Brettel & Witt, 1983). But, as shown in Tables 2 and 3, this is not the case. Instead, there is a corresponding increase in the 1, 5, and 35 μs kinetic components for both EG- and EGW-treated samples. The 35 μs component has been suggested to arise from perturbed PSII centers, the nature of which is unknown (Schlodder & Mayer, 1987; Hoganson et al., 1991). In the presence of EG the 35 μs component exhibits an amplitude increase and then a decrease with increasing EG concentrations (Table 2) where the maximum occurs over the 40−90% range and represents nearly 30% of the total signal. A similar trend is observed for the EGW-treated samples (Table 3), although in this case the decline of this component around 60% EG appears to be associated with an increase in the 1 μs component.

A microsecond component of 5 ± 3 μs has been observed in previous analyses of the $P680^+$ reduction kinetics (Brettel & Witt, 1983; Schlodder et al., 1985) and attributed to an unidentified intrinsic donor to $P680^+$ (Conjeaud et al., 1979; Conjeaud & Mathis, 1980). In our measurements, the 5 μs component is only apparent in the presence of EG, having a negligible contribution in control and EGW-treated samples. In the range of 40−80% EG, the contribution of this component amounts to as much as 40% of the total signal amplitude. It is unclear why the 5 μs component is induced by the presence of EG, but these results do suggest that this is due to a direct solvent interaction.

In contrast to the 5 and 35 μs components, the 1.0 ± 0.1 μs component contributes up to 50% of the total signal amplitude in the presence of 40−80% EG. For the samples returned to the standard buffer medium, a similar contribution is observed. However, in control samples, the 1 μs component represents only ∼10% of the total signal amplitude.

Finally, an interesting finding was that at very high EG concentrations (>95%) the 830 nm absorption signal changed sign. The signal decreases to zero at about 95% EG and then becomes negative as the EG concentration is further increased. This phenomenon is shown at the bottom of Figure 5 for a sample in 98% EG where the negative signal reaches a maximum amplitude of ∼−0.3 relative to the untreated control. A 3 μs rise time and a two-component recovery with decay times of ∼30 and ∼100 μs could be fitted to the relevant transient in Figure 5. Upon return of the sample to the standard buffer medium, the negative signal was still retained but the absorption rise time became shorter (<1 ns) and the decay comprised only a single component of ∼100 μs (Figure 5). This would indicate that there are at least two contributions to the negative signal and that the contributions which correspond to the 3 μs rise and the 30 μs decay are specifically induced by EG. The concentration dependence of this signal over the 95−99% EG range was highly sensitive to the precise EG concentration. This may suggest a competition between EG and water for solvation of PSII. Earlier it was observed that at the high EG concentrations selected xanthophyll pigments are extracted (Hillier et al., 1992). To ensure that the negative absorption change was not associated with free pigments, a supernatant fraction from a 99% EG sample was measured. No 830 nm signal was found in the yellow supernatant. A possible explanation for these observations may be the formation of EG-solvated chlorophyll triplet states in PSII.

DISCUSSION

The exposure of PSII membrane fragments to increasing EG concentrations results in both solvent-induced electronic effects and gross protein structural changes. Three broad concentration regions can be identified where these effects occur: (1) low EG concentrations (30−60%) where there are reversible changes in the Q_A^- recombination and $P680^+$ reduction kinetics; (2) intermediate EG concentrations (50−70%) where protein structural changes occur that lead to the release of the extrinsic proteins, destabilization of two of the catalytic Mn ions, inactivation of O_2 evolution, and increase in donor-side H_2O_2 formation; and (3) high EG

concentrations (>70%) where there is an irreversible loss of PSII photochemistry and the apparent formation of new deactivation pathways.

Solvent-Induced Effects. Under mixed-solvent conditions, EG appears to have specific, reversible effects on the electronic and energy transfer events in PSII. In the 30−60% EG range, there is a reversible slowing in the Q_A^- recombination kinetics (Table 1) as well as a reversible loss in the nanosecond kinetics for $P680^+$ reduction (Figure 6). One possible explanation for these effects may be that EG causes a lowering of the midpoint potentials of the intermediate S_n states and/or of the electron acceptor side (Malkin, 1981). Earlier work has shown, for example, that the S_2 state in PSII samples prepared without the 33 kDa protein (Miyao et al., 1987) and in 33 kDa (*psb*O) deletion mutants (Philbrick et al., 1991; Burnap et al., 1992) has a much higher stability, presumably because of altered solvent interactions. However, the reversible effects on Q_A^- reoxidation and $P680^+$ reduction occur for the most part before EG causes the release of the extrinsic proteins and the catalytic Mn (Figure 2).

Alternatively, the above reversible effects may be due to a blockage of S_n-state cycling through substrate limitation. However, were this the case, it would have to involve a local microconformational phenomenon that alters solvent accessibity since at ∼50% EG the concentration of bulk water still remains high at ∼30 M. A reversible loss in the nanosecond kinetics for $P680^+$ reduction has been documented earlier for acetate-treated PSII samples (Saygin et al., 1986). The mechanism under this condition was suggested to be the replacement of Cl^- as a catalytic cofactor in the OEC by acetate. However, the involvement of Cl^- ions in the OEC reactions is complicated (Wydrzynski et al., 1990; Lindberg et al., 1993), and in our work no attempt was made to purposely deplete the sample of chloride which was sufficiently present in the standard buffer medium. It may be that the reversible losses in the nanosecond kinetics after either chloride depletion or EG treatment are due to microconformational changes. More experimental work is required to clarify this point.

A second solvent-specific effect is observed at higher EG concentrations (60−90%), after O_2 evolution has been inactivated, and is indicated by the appearance of a 5 μs decay component in the $P680^+$ reduction kinetics (Tables 2 and 3) and the simultaneous rise in the F_O fluorescence level (Figure 3B). Both of these effects are also reversed upon return of the sample to the standard buffer medium. The 5 μs component could represent the formation of a new deactivation pathway for $P680^+$ or may arise from the formation of another species with an absorption at 830 nm such as ^{3}Chl or carotenoid cations (Reinman & Mathis, 1981; Schlodder et al., 1985). Although the generation of an alternate species is likely to occur under conditions when electron transfer from water becomes blocked, the results, particularly the change in the F_O level, may indicate that the pigment bed becomes disconnected from the reaction center. Again, future work will be needed, particularly to determine the wavelength dependence of the kinetic changes, in order to clarify the molecular mechanism involved.

Protein Structural Changes. Upon the exposure of PSII samples to EG concentrations in the region 50−70%, the 16, 23, and 33 kDa extrinsic proteins are released (Figure 2A) and O_2 evolution is inactivated (Figure 1). The inhibition of O_2 evolution occurs over a narrow concentration range and is similar to the effect of protein denaturation by thermal inactivation (Thompson et al., 1989; Williams & Gounaris, 1993). Typically, the extrinsic proteins are released by the addition of high concentrations of divalent cations or chaotropic agents (Andersson & Åkerlund, 1987), and it is believed that the binding of these proteins occurs largely through electrostatic forces. EG, an electrically neutral molecule, may cause the release of the extrinsic proteins, and subsequently the Mn, by a weakening of the electrostatic and H-bonding interactions through its effect on the dielectric of the suspending medium.

The release of the extrinsic proteins by EG is, however, variable. In particular, in 80−100% EG only a partial release of the three proteins occurs (Figure 2A), and at 100% EG the release of the 16 and 33 kDa proteins takes place without any apparent loss of the 23 kDa protein (Figure 2A). Currently, it is not known whether the 16 and 23 kDa proteins bind to the 33 kDa protein or to intrinsic polypeptides of the PSII complex. Earlier work has suggested that the binding of the 33 kDa protein creates a conformational site for the binding of the 23 kDa protein (Miyao & Murata, 1989). But our results demonstrate that the 23 kDa protein can bind to the intrinsic core of PSII in the absence of the 33 kDa protein. Recent studies on the effects of mercury on PSII also indicate that the 33 kDa protein can be released without the removal of the 23 kDa protein (Bernier & Carpentier, 1995). The differential binding of the extrinsic proteins at the high EG concentrations clearly suggests that changes in the binding affinities are responsible for their association and that this is strongly influenced by solute/solvent interactions.

The release of the extrinsic proteins, particularly the 33 kDa protein, is typically correlated with a loss of functional Mn ions from PSII (Ono & Inoue, 1984; Miyao & Murata, 1984). In this work, we also observe a similar correlation upon EG treatment (Figure 2B). However, only two Mn ions are lost over the intermediate EG concentration range, suggesting that two Mn ions in the catalytic cluster of four are bound more strongly or are located in a chemically different environment as has been suggested earlier (Kambara & Govindjee, 1985). Regardless, EG treatment does not appear to interfere with the tightly-bound Mn ions since under this condition PSII electron transport can still occur from an artificial donor (Figure 1). More importantly, at high EG concentrations more than two Mn ions remain bound. Usually, during normal biochemical isolation procedures, it is considered that the bound Mn ions become reduced which destabilizes their ligation to the protein. In previous attempts to isolate Mn binding proteins, chemical oxidants were employed to prevent this reduction (Abramowicz & Dismukes, 1984; Yamamoto et al., 1984). But in this situation, Mn ions were found to become associated with the extrinsic 33 kDa protein, which is known not to bind the functional Mn (Ono & Inoue, 1983). In this work we have no data to determine what protein the loosely-bound Mn may be associated with, but propose that EG may be a practical solvent for localizing the Mn ions in the protein domain.

Earlier it was reported that upon the loss of the extrinsic proteins by salt treatment, alternate water oxidation products in the form of H_2O_2 can be detected (Hillier et al., 1993). A similar effect is observed after EG treatment where the

observed rate of donor-side H_2O_2 generation increases as much as 6-fold (Figure 1). As in the earlier work, the increase in H_2O_2 formation occurs at the expense of O_2 evolution and may explain the source of electrons for Q_A reduction and the high F_V/F_M values (Figure 3A). A similar observation was made for lauroylcholine-treated thylakoid and PSII samples (Wydrzynski et al., 1985, 1996).

Reduced Water Concentrations. PSII samples treated at very high EG concentrations (>70%) undergo a loss in primary photochemistry as reflected in the decline of both the 830 nm absorption signal (Figures 5 and 6) and the DPC-DCPIP reaction (Figure 1). This inactivation is irreversible as there is no restoration of activity upon return of the sample to the standard buffer medium. The loss of charge separation indicates irreversible changes to PSII, even though most of the chlorophyll is retained under this condition (Hillier et al., 1992). However, there may be the loss of other essential PSII components. Preliminary analysis indicates that high EG concentrations do extract some of the lipids (data not shown), and earlier work by Jordan et al. (1983) and Eckert et al. (1987) suggests that lipids play an important role in the charge separation process.

Alternatively, the irreversible loss in activity under very high EG concentrations (>95%) may be due to much lower water concentrations, where changes in solute/solvent interactions cause irreversible protein denaturation. If this is so, then the question arises as to why the loss of activity is not reversible since lyophilized PSII samples can be restored upon return to aqueous media with minimal effect on the total activity (Kawamoto & Asada, 1990; Hillier, unpublished results). Our observations may be related to the degree of dehydration that takes place in the various treatments. For many proteins, water molecules serve as direct ligands (Timasheff, 1992) with some being very tightly bound. If this tightly-bound fraction is removed, the protein denatures and loses enzymatic activity (Klibanov, 1989). Thus, at the very high concentrations of EG there may be a greater loss of tightly-bound water through mass action, resulting in conformational changes that remain largely irreversible in the rapid solvent replacement and rehydration processes that we used. Nevertheless, it is important to point out that EG treatment does not result in gross dissociation of the PSII complex as evident by the protein SDS−PAGE pattern and the retention of bound chlorophyll in 100% EG (Hillier et al., 1992). The denaturation under high EG conditions may therefore be occurring in peripheral regions of the PSII complex rather than in the transmembrane regions (Haltia & Freire, 1995).

The development of a nonaqueous solvent system for the manipulation of PSII would provide a valuable experimental system. It would allow one to address fundamental questions regarding substrate affinity and specificity in the water oxidation mechanism. In addition, it could provide a means to localize a Mn binding domain in PSII. In this paper, we have identified solvent-induced electronic and structural effects on PSII by ethylene glycol. More work is needed to determine the effects of ethylene glycol in combination with other stabilizing conditions of PSII, such as the addition of glycine betaine (Papageorgiou & Murata, 1995) and the use of lower temperatures. Preliminary results in our laboratory indicate that these conditions do indeed reduce the denaturing effects of EG at high concentrations. This will be the subject of a future publication.

ACKNOWLEDGMENT

We would like to thank M. Ghirardi and T. Lutton for their assistance with the flash probe fluorescence measurements.

REFERENCES

Abramowicz, D. A., & Dismukes, G. C. (1984) *Biochim. Biophys. Acta 765,* 309−318.
Andersson, B. & Åkerlund, H-E. (1987) in *Topics in Photosynthesis* (Barber, J. Ed.) Vol. 8, pp 379−420, Elsevier, Amsterdam.
Apostolova, E., Busheva, M., & Tenchov, B. (1995) *Photosynthetica 30,* 475−479.
Armstrong, J. McD. (1964) *Biochim. Biophys. Acta 86,* 194−197.
Berg, S. P., & Seibert, M. (1987) *Photosynth. Res. 13,* 3−17.
Bernier, M., & Carpentier, R. (1995) *FEBS Lett. 360,* 251−254.
Berthold, D. A., Babcock, G. T., & Yocum, C. F. (1981) *FEBS Lett. 134,* 231−234.
Boerner, R. J., Nguyen, A. P., Barry, B. A., & Debus, R. J. (1992) *Biochemistry 31,* 6660−6672.
Brettel, K., & Witt, H. T. (1983) *Photobiochem. Photobiophys. 6,* 253−260.
Brettel, K., Schlodder, E., & Witt, H. T. (1984) *Biochim. Biophys. Acta 766,* 403−415.
Bricker, T. M. (1992) *Biochemistry 31,* 4623−4628.
Burnap, R. L., Shen, J.-R., Jursinic, P. A., Inoue, Y., & Sherman, L. (1992) *Biochemistry 31,* 7404−7410.
Buser, C. A., Diner, B. A., & Brudvig, G. W. (1992) *Biochemistry 31,* 11449−11459.
Chu, H.-A., Nguyen, A. P., & Debus, R. J. (1994a) *Biochemistry 33,* 6137−6149.
Chu, H.-A., Nguyen, A. P., & Debus, R. J. (1994b) *Biochemistry 33,* 6150−6157.
Chu, H.-A., Nguyen, A. P., & Debus, R. J. (1995a) *Biochemistry 34,* 5839−5858.
Chu, H.-A., Nguyen, A. P., & Debus, R. J. (1995b) *Biochemistry 34,* 5859−5882.
Conjeaud, H., & Mathis, P. (1980) *Biochim. Biophys. Acta 590,* 353−359.
Conjeaud, H., & Mathis, P. (1986) *Biophys. J. 49,* 1215−1221.
Conjeaud, H., Mathis, P., & Paillotin, G. (1979) *Biochim. Biophys. Acta 546,* 280−291.
Dau, H. (1994) *Photochem. Photobiol. 60,* 1−23.
Debus, R. J. (1992) *Biochim. Biophys. Acta 1102,* 269−352.
Dordick, J. S. (1989) *Enzyme. Microb. Technol. 11,*194−222.
Eckert, H.-J., Toyoshima, Y., Akabori, K., & Dismukes, G. C. (1987) *Photosynth. Res. 14,* 31−41.
Farkas, D. L., & Malkin, S. (1979) *Plant Physiol. 64,* 942−947.
Ghirardi, M. L., Lutton, T. W., & Seibert, M. (1996) *Biochemistry 35,* 1820−1828.
Haltai, T., & Freire, E. (1995) *Biochim. Biophys. Acta 1228,* 1−27.
Hansson, Ö., & Wydrzynski, T. (1990) *Photosynth. Res. 23,* 131−162.
Hillier, W., & Wydrzynski, T. (1993) *Photosynth. Res. 38,* 417−423.
Hillier, W., Wydrzynski, T., & Seibert, M. (1992) in *Research in Photosynthesis* N., (Murata, Ed.) Vol. II, pp 167−170, Kluwer Academic Publishers, Dordrecht.
Hoganson, C. W., Casey, P. A., & Hansson Ö. (1991) *Biochim. Biophys. Acta 1057,* 399−406.
Ikeuchi, M., & Inoue, Y. (1988) *Plant Cell Physiol. 29,* 1233−1239.
Inoue, H., & Nishimura, M. (1971) *Plant Cell Physiol. 12,* 137−145.
Joliot, P. (1968) *Photochem. Photobiol. 8,* 451−463.
Jordan, B. R., Chow, W.-S., & Baker, A. (1983) *Biochim. Biophys. Acta 725,* 77−86.
Kawamoto, K., & Asada, K. (1990) in *Research in Photosynthesis* (Baltscheffsky, M., Ed.) Vol. I, pp 889−892, Kluwer Academic Publishers, Dordrecht.
Klibanov, A. M. (1989) *Trends Biol. Sci. 14,* 141−144.
Kok, B., Forbush, B., & McGloin, M. (1970) *Photochem. Photobiol. 11,* 457−475.

Kuwabara, T., & Murata, N. (1982) *Plant Cell Physiol. 23*, 533−539.
Lindberg, K., Vänngård, T., & Andréasson, L.-E. (1993) *Photosynth. Res. 38*, 401−408.
Lukins, P. B., Post, A., Walker, P. J., & Larkum, A. W. D. (1996) *Photosynth. Res.* (in press).
Malkin, S. (1981) *Isr. J. Chem. 21*, 306−315.
Mauzerall, D. (1972) *Proc. Natl. Acad. Sci. U.S.A. 69*, 1357−1362.
Messinger, J., Badger, M., & Wydrzynski, T. (1994) *Proc. Natl. Acad. Sci. U.S.A. 92*, 3209−3213.
Meyer, B., Schlodder, E., Dekker, J. P., & Witt, H. T. (1989) *Biochim. Biophys. Acta 974*, 36−43.
Miyao, M., & Murata, N. (1984) *FEBS Lett. 170*, 350−354.
Miyao, M., & Murata, N. (1989) *Biochim. Biophys. Acta 977*, 315−321.
Miyao, M., Murata, N., Lavorel, L., Maison-Peteri, B., Boussac, A., & Etienne, A.-L. (1987) *Biochim. Biophys. Acta 890*, 151−159.
Nixon, P. J., & Diner, B. A. (1992) *Biochemistry 31*, 942−948.
Nuijs, A. M., van Gorkom, H. J., Plijter, J. J., & Duysens, L. N. M. (1986) *Biochim. Biophys. Acta 848*, 167−175.
Ono, T.-A., & Inoue, Y. (1983) *FEBS Lett. 164*, 255−259.
Ono, T.-A., & Inoue, Y. (1984) *FEBS Lett. 168*, 281−286.
Osmond, C. B. (1994) in *Photoinhibition: molecular mechanisms to the field* (Baker, N. R., Ed.) pp 1−24, Bios Scientific Publications, Oxford.
Papageorgiou, G. C., & Murata, N. (1995) *Photosynth. Res. 44*, 243−252.
Philbrick, J. B., Diner, B. A., & Zilinskas, B. A. (1991) *J. Biol. Chem. 266*, 13370−13376.
Pokorny, A., Wulf, K., & Trissl. H.-W. (1994) *Biochim. Biophys. Acta 1184*, 65−70.
Preston, C., & Seibert, M. (1991a) *Biochemistry 30*, 9615−9624.
Preston, C., & Seibert, M. (1991b) *Biochemistry 30*, 9625−9633.
Reinman, S., & Mathis, P. (1981) *Biochim. Biophys. Acta 635*, 249−258.
Robinson, H. H., & Crofts, A. R. (1983) *FEBS Lett. 153*, 221−226.
Roelofs, T. A., Lee., C.-H., & Holzworth, A. R. (1992) *Biophys. J. 61*, 1147−1163.
Saygin, Ö., Gerken, S., Meyer, B., & Witt, H. T. (1986) *Photosynth. Res. 9*, 71−78.
Schatz, S. H., Brock, H., & Holzwarth, A. R. (1987) *Proc. Natl. Acad. Sci. U.S.A. 84*, 8414−8418.
Schatz, S. H., Brock, H., & Holzwarth, A. R. (1988) *Biophysical Journal 54*, 397−405.
Schlodder, E., & Meyer, B. (1987) *Biochim. Biophys. Acta 890*, 23−31.
Schlodder, E., Brettel, K., & Witt, H. T. (1985) *Biochim. Biophys. Acta 808*, 123−131.
Schröder, W. P., & Åkerlund, H.-E. (1986) *Biochim. Biophys. Acta 848*, 359−363.
Seibert, M. (1993) in *The Photosynthetic Reaction Center* (Deisenhoffer, J., Norris, J. R., Eds.) Vol. 1, pp 319−356, Academic Press, New York.
Seibert, M., Cotton, T. M., & Metz, J. G. (1988) *Biochim. Biophys. Acta 934*, 235−246.
Seibert, M., Tamura, N., & Inoue, Y. (1989) *Biochim. Biophys. Acta 974*, 185−191.
Smith, P. J., & Pace, R. J. (1996) *Biochim. Biophys. Acta 1275*, 213−220.
Stewart, A. C., & Bendall, D. S. (1981) *Biochem. J. 194*, 877−887.
Thompson, L. K., Miller, A.-F., Buser, C. A., de Paula, J. C., & Brudvig, G. W. (1989) *Biochemistry 28*, 8048−8056.
Timasheff, S. N. (1992) *Biochemistry 31*, 9857−9864.
Van Gorkom, H. J., Pulles, M. P. J., & Wessels, J. S. C. (1975) *Biochim. Biophys. Acta 408*, 331−339.
Van Best, J. A., & Mathis, P. (1978) *Biochim. Biophys. Acta 503*, 178−188.
Van Mieghem, F., Brettel, K., Hillmann, B., Kamlowski, A., Rutherford, W. A., & Schlodder, E. (1995) *Biochemistry 34*, 4798−4813.
Völker, M., Eckert, H.-J., & Renger, G. (1987) *Biochim. Biophys. Acta 890*, 66−76.
Waiselewski, M. R., Johnson, D. G., Seibert, M., & Govindjee (1989) *Proc. Natl. Acad. Sci. U.S.A. 86*, 524−528.
Williams, W. P., & Gounaris, K. (1992) *Biochim. Biophys. Acta 1100*, 92−97.
Wydrzynski, T., Huggins, B. J., & Jursinic, P. A. (1985) *Biochim. Biophys. Acta 809*, 125−136.
Wydrzynski, T., Baumgart, F., MacMillan, F., & Renger, G. (1990) *Photosynth. Res. 25*, 59−72.
Wydrzynski, T., Hillier, W., & Messinger, J. (1996) *Physiol. Plant. 96*, 342−350.
Yachandra, V. K., DeRose, V. J., Latimer, M. J., Mukerji, I., Sauer, K., & Klein, M. P. (1993) *Science 260*, 675−697.
Yamamoto, Y., Doi, M., Tamura, W., & Nishimura, M. (1981) *FEBS Lett. 113*, 265−268.
Yamamoto, Y., Shinkai, H., Isogai, Y., Matsuura, M., & Nishimura, M. (1984) *FEBS Lett. 175*, 429−432.
Zacs, A., & Klibanov, A. M. (1985) *Proc. Natl. Acad. Sci. U.S.A. 82*, 3192−3196.

BI961724J